Photochemistry and Photobiology, 20**, **: *–*

Research Article

A Highly Selective and Sensitive Colorimetric Chemosensor for the Detection of Hydrogen Sulfide: A Real-ftime Application in Multiple platforms

Dhanapal Jothi[1], Sathishkumar Munusamy[2] and Sathiyanarayanan Kulathu Iyer[1]*

[1]Department of Chemistry, School of Advanced Sciences, Vellore Institute of Technology, Vellore, India
[2]Institute of Chemical Biology and Nanomedicine, State Key Laboratory of Chemo/Bio-sensing and Chemometrics, College of Chemistry and Chemical Engineering, Hunan University, Changsha, China

Received 2 May 2021, accepted 10 August 2021, DOI: 10.1111/php.13506

ABSTRACT

Calorimetric chemosensors are found to be advantageous sensing systems due to their simplicity and favorable responsive properties. Although some colorimetric probes have been reported to detect hydrogen sulfide (H_2S), the creation of rapid, highly selective and sensitive probes for the detection of H_2S remains a challenging target. In this work, we established dinitrosulphonamide decorated phenanthridine and 2,4-dinitro-N-(4-(7,8,13,14-tetrahydrodibenzo[a, i]phenanthridin-5-yl)phenyl)benzenesulfonamide (PHSH), for the calorimetric detection of H_2S. H_2S-triggered thiolysis of PHSH resulted in a marked absorption enhancement alongside a visual color change from colorless to dark yellow. The result indicated that the chemosensor showed high sensitivity and selectivity with a fast response of less than 10 s with a detection limit as low as 6.5 nM. The chemosensor reaction mechanism with H_2S was studied by UV-vis, ^{1}H NMR, mass and HPLC analysis. In addition, the chemosensor has been used for the determination of H_2S in many real-time samples.

INTRODUCTION

Since the industrial revolution, there has been an uninterrupted pile up of toxic and dangerous gaseous pollutants in the environment. Among them, hydrogen sulfide (H_2S) has been broadly studied for its known environmental hazard. Industrial production of natural gas, biogas and mining are the primary contributors to the ecological release of H_2S. In particular, H_2S in biogas can range up to 10–2000 ppm, a nuisance with no energy value and an impediment that acts like poison for catalyst and as corrosive agent. As a water-soluble gas, H_2S, in industrial wastewater, exudes not only a foul smell resembling "rotten eggs" (1) but also instills a severe threat to human health when humans consume H_2S-contaminated water and food (2). Besides, H_2S is an unwelcoming component of wine, as it negatively contributes to the quality of wine, which incurs significant economic losses (3–5). Again, from the physiological point of view, H_2S is a vital gasotransmitter next only to nitric oxide (NO) and carbon monoxide (CO). Though H_2S contributes to many biological processes, abysmal metabolism of H_2S can be associated with an array of diseases such as Alzheimer's disease (6), Down's syndrome (7), diabetes (8) and liver cirrhosis (9), which necessitates the in vivo detection of H_2S. Given the inevitable role of H_2S as an environmental pollutant and in biological processes, early detection could ameliorate the dreadful impact of H_2S.

In recent years, with the ongoing efforts of research groups, various methods have been developed to detect H_2S. For example, electrochemical assays (10–14), chromatography (15–17), metal-induced sulfide precipitation (18) and optical probes are the main techniques to detect H_2S. Among these methods, optical detection has received significant attention in recent years owing to its simplicity, high sensitivity and selectivity, and good repeatability (19–38). Chemodosimeter is the most common optical approach in which the chemical probe is incorporated with an H_2S selective irreversible responsive unit and optical response modulator. Functional groups such as nitro (39–41), azide (42–48), hydroxylamine (49) (H_2S induced reduction), dinitrophenyl ethers (50–60), disulfide bonds (61), nitrobenzoxadiazole ether (62, 63) and nitrobenzofurazan (64–68) (NBD) (H_2S induced hydrolysis) are the functional groups dexterously employed for the detection of H_2S. As H_2S has a strong binding affinity toward metal ions, its metal displacement or coordination has also been copiously used to detect H_2S (69, 70). Though most of the optical techniques to detect H_2S are based on fluorescence changes, visible color change of the probes in the presence of H_2S is also often reported.

Sensors based on the colorimetric approach are gaining substantial interest as they offer instantaneous detection of analyte and visually detectable color change. With these valuable traits, colorimetric systems can monitor the H_2S emission levels in the target industrial platforms and can be employed in geological monitoring. Nevertheless, the research on the development of selective and sensitive chromogenic probes to detect H_2S is inadequate. As part of our ongoing interest in developing optical sensors for important analytes (71–75), in this work, we developed a simple phenanthridine-based colorimetric probe to detect H_2S. In the design of this probe, phenanthridine was incorporated with the 2,4-dinitrobenzene sulfonyl (DNBS) group, a widely used selective signaling unit for H_2S. On the other hand, phenanthridine is a simple chromogenic molecule with outstanding

*Corresponding author email: sathiya_kuna@hotmail.com (Sathiyanarayanan Kulathu Iyer)

advantages of straightforward synthesis, intriguing optical property and easy functionalization. To our surprise, the colorimetric H_2S sensor derived from DNBS was conspicuously uncommon. Moreover, sensor **PHSH** could detect H_2S in multiple real-time geological and industrial samples such as wastewater and wine.

MATERIALS AND METHODS

All the chemical reagents and organic solvents were purchased as AR and LR grade from commercial sources and used without further purification. The compound purifications were done by column chromatography using 100-200 mesh silica gel. ^1H NMR and ^{13}C NMR spectra were recorded on a Bruker 400 MHz NMR spectrometer using tetramethylsilane (TMS) as an internal standard. HRMS results were acquired from Joel GC Mate II GC-Mass spectrometer. Electronic absorption spectra were recorded with a Hitachi-2910 UV-Vis spectrophotometer.

Synthesis of 4-(7,8,13,14-tetrahydrodibenzo[a,i]phenanthridine-5-yl) aniline (PHN). 4-(7,8,13,14-tetrahydrodibenzo[a,i]phenanthridine-5-yl) aniline **(PHN)** was prepared based on a previous literature procedure [92]. Yield: 70%, HRMS (ESI) *m/z*: Calcd for $C_{27}H_{22}N_2$ 374.1783; Found: 374.1769. ^{1}H NMR(400MHz, DMSO-*d6*)^{TM}: δ 2.702-2.717 (t, 2H, J = 6 Hz), 2.896-2.902 (d, 4H, J = 2.4 Hz), 3.033-3.050 (t, 2H, J = 6.8 Hz), 6.702-6.723 (d, 2H, J = 8.4 Hz), 6.850-6.868 (m, 2H, J = 7.2 Hz), 7.124-7.126 (m, 3H, J = 0.8 Hz), 7.291-7.297 (m, 3H, J = 2.4 Hz), 7.383-7.388 (m, 1H, J = 2 Hz), 7.578-7.595 (t, 1H, J = 6.8 Hz) and 9.658 (s, 2H, NH_2). ^{13}C NMR (DMSO-*d6*, 100 MHz): δ 29.07, 29.17, 29.21, 33.07, 115.37, 125.83, 126.67, 126.79, 127.35, 127.56, 128.13, 128.27, 128.35, 129.08, 129.18, 131.38, 132.82, 132.92, 133.34, 139.11, 139.47, 145.97, 153.70, 157.55 and 157.80.

Synthesis of 2,4-dinitro-N-(4-(7,8,13,14-tetrahydrodibenzo[a,i] phenanthridine-5-yl)phenyl)benzenesulfonamide (PHSH). Compound 4-(7,8,13,14-tetrahydrodibenzo[a,i]phenanthridine-5-yl) aniline **(PHSH)** (1 g, 0.00267 mmol) was clearly dissolved in 10 mL of CH_2Cl_2, and Et_3N (0.577 mL, 0.004 mmol) was added dropwise. Finally, 2,4-Dinitrosulfonyl chloride (0.852 mg, 0.0032 mmol) was charged into the reaction mixture solution. The resulting crude mixture was stirred at room temperature for 9 h, and the completion of the reaction was monitored by TLC. The crude residue was purified by column chromatography (eluent n-hexane/ethyl acetate ratio 8:2) to give the light-yellow color solid, m.p 218°C HRMS (ESI) *m/z*: Calcd for $C_{33}H_{24}N_4O_6S$ 604.1417; Found: 604.1279. ^{1}H NMR (400 MHz, DMSO-d_6)^{TM}: *δ* 2.721-2.735 (d, 2H, J = 5.6 Hz), 2.906-2.915 (d, 4H, J = 6 Hz), 3.057-3.073 (t, 2H, J = 6.4 Hz), 6.682-6.702 (d, 1H, J = 8), 6.941-6.959 (t, 1H, J = 7.2 Hz), 7.143-7.163 (d, 3H, J = 8 Hz), 7.298-7.316(m, 3H, J = 7.2 Hz), 7.402-7.422 (d, 3H, J = 8 Hz), 7.594-7.606 (d, 1H, J = 4.8 Hz), 8.279-8.301 (d, 1H, J = 8.8 Hz, 8.642-8.664 (d, 1H, J = 8.8 Hz and 9.142 (s, NH). ^{13}C NMR (DMSO-d_6, 100MHz): δ 28.90, 29.04, 29.10, 121.59, 122.28, 126.03, 126.69, 127.69, 127.73, 127.78, 127.82, 128.32, 128.42, 129.00, 129.21, 129.42, 131.06, 132.18, 132.48, 132.55, 134.21, 139.36, 139.57, 142.27, 146.23, 148.39, 148.65, 151.89, 151.95 and 158.07.

Stock solution preparation. A stock solution of **PHSH** (2×10^{-5} M) was prepared in acetonitrile: water (7:3, v/v) solvent medium. All the solutions of anions and ligands (0.2 M) were prepared in PBS buffer solution (pH = 7.4). The change in absorbance was monitored at 435 nm.

Preparation of test paper strip. To investigate real-time analyses of cellulose-based test paper (Whatman, Grade 1, US), a probe of 20 μM solution was prepared in acetonitrile solvent. Test papers were immersed in probe solution followed by air drying at room temperature. **PHSH**-coated test paper strips were dipped into various anion solutions to detect the anions. Color changes were captured with a digital camera.

H_2S detection in real water samples. The water samples, including the tap water, well water and lake water collected from in and around Vellore Institute of Technology, Vellore, were filtered through a 0.20-μm pore size membrane filter to remove suspended particulate matters. Red wine and beer samples were acquired from commercial sources and used as such. The collected samples were mixed with the **PHSH** stock solution, and the final ratio was acetonitrile/sample (v/v = 70:30) for the test of real water samples. After that, different amounts of H_2S were added to the real-time samples. Finally, the results were tested by the absorbance measurements. The data were calculated as the average of three separate measurements.

RESULTS AND DISCUSSION

Design and synthesis of PHSH

The above-mentioned concerns inspired us to build a colorimetric probe for monitoring H_2S with ultra-sensitivity. We opted for phenanthridine core as they exhibit excellent optical property, structural stability and easy maneuvers for switching signals. The key to developing the optical probe for H_2S is to judiciously incorporate an appropriate H_2S signaling unit into the probe. Ideally, such a functional group should react only with H_2S but not with other sulfur species and anions. In this study, we opted for the 2,4-dinitrobenzene sulfonyl (DNBS) group as the H_2S signaling group. Thiolysis of DNBS has many advantages, such as the ability of DNBS to be attached to the central core by single-step reaction, diminishment of optical property due to the presence of the nitro group and its high selectivity toward H_2S than other competitive thiols, for example, glutathione and cysteine (Cys). Following these rationales, we herein designed and synthesized the **PHSH** (see Scheme 1) as a new probe for the selective colorimetric detection of hydrogen sulfide. We started our work by synthesizing 4-(7,8,13,14-tetrahydrodibenzo[a, i]phenanthridin-5-yl)aniline (PHN) from 2-tetralone and 4-amino benzaldehyde using the previously reported procedure by our group (76). Then, the synthesis of **PHSH** was realized by reaction between (PHN) and DNBS. Notably, both reactions proceeded efficiently under simple reaction conditions with good yields. The molecular structure of the probe **PHSH** was thoroughly confirmed by ^{1}H and ^{13}C NMR and HRMS analyses (see the Supporting Information for full details).

Visual observation

As a preliminary confirmation, the colorimetric sensitivity of **PHSH** (2 x 10^{-5} M) toward various anions was studied. Various anionic solutions were added separately (2 equiv.) to the sensor solution, and the color change was observed visually. As shown in Fig. 1a, upon the addition of H_2S to the solution of **PHSH**, a sudden color change from transparent to dark yellow was observed. However, the solution **PHSH** remained transparent over the addition of other competitive anions. In addition, the color change of **PHSH** from translucent to dark yellow was gradual with increasing concentration of H_2S (Fig. 1b). Hence, without the need for customary complex instrumentation, initial H_2S analysis can be made using **PHSH** by simple visualization.

Absorption spectral studies of PHSH with H_2S

High photostability is an essential attribute of a chemosensor for sustainable utilization in chemical and biological experiments. Hence, time-dependent absorption studies were carried out by irradiating the solution of **PHSH** with UV light (254 nm). The absorption spectra of **PHSH** remained almost unaffected upon the UV irradiation for about 60 min (Figure S4), which indicates that **PHSH** is highly photostable.

The UV-vis studies of **PHSH** were carried out with 2 X 10^{-6} M sensor solution prepared in acetonitrile: water (7:3)

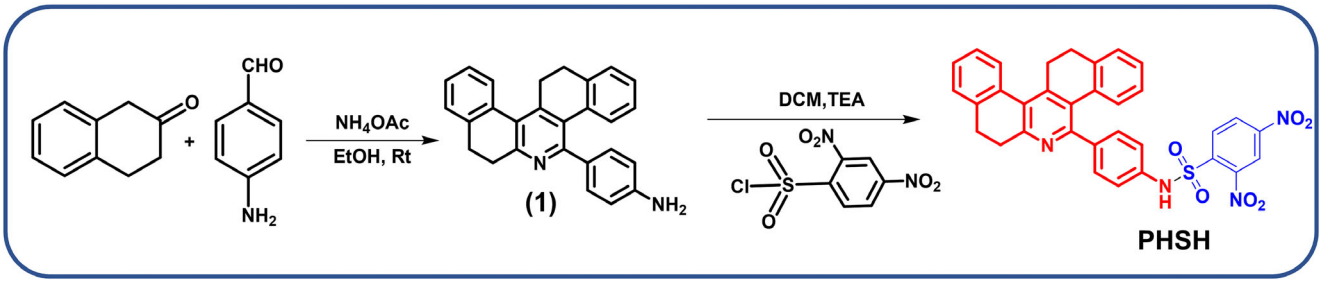

Scheme 1. Schematic representation of the synthesis of sensor **PHBS**.

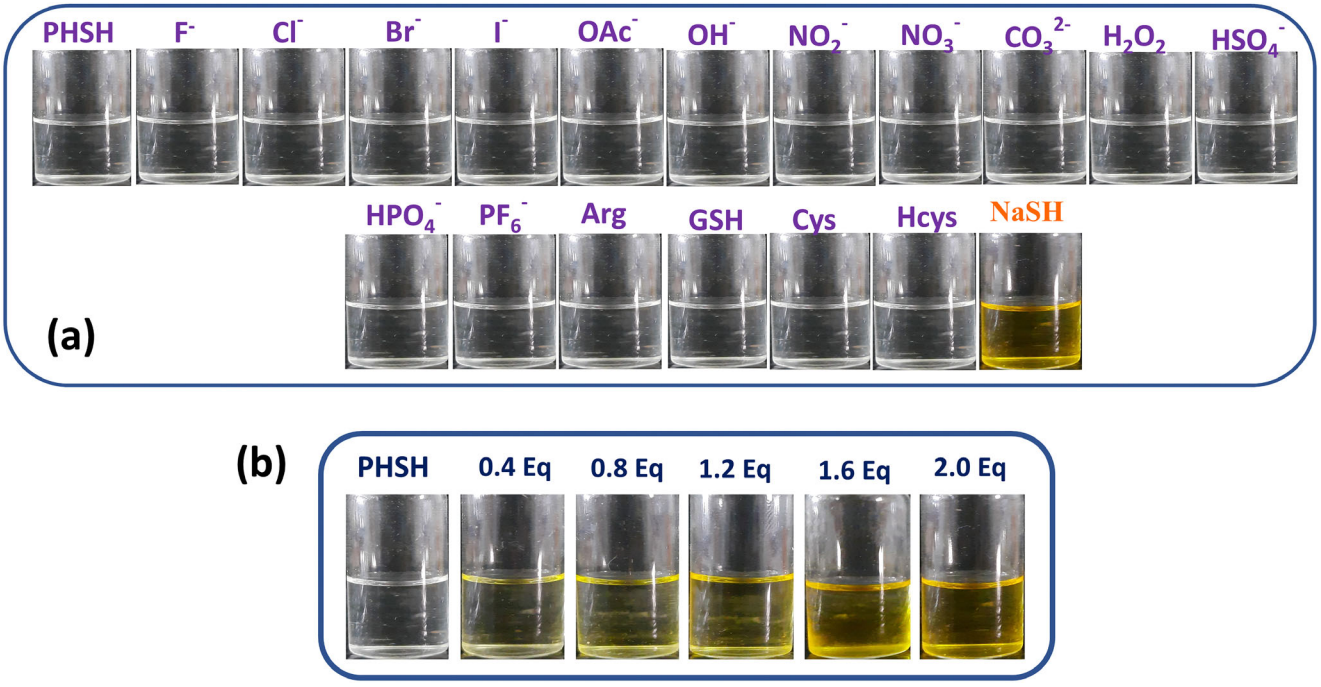

Figure 1. (a) Colorimetric response of **PHBS** (2×10^{-5} M) in acetonitrile solution upon addition of 2 equivalents of various anions. (b) Visible color change of **PHBS** upon addition of increasing concentration of H_2S.

solvent medium. Free **PHSH** showed a single absorption peak at the wavelength of 315 nm (ε = 13 000 M^{-1} cm^{-1}), which could be corroborated to π-π^* electron transition. Upon adding H_2S (2 equiv.), a new absorption peak emerged at the wavelength of 435 nm (ε = 18 500 M^{-1} cm^{-1}) with diminution of absorption at 315 nm. The formation of a significant red-shifted new absorption peak for the sensor indicates the newly formed product's enhanced internal charge transfer (ICT). The sensing ability of **PHSH** was also checked with other competing anions and ligands, such as F^-, Cl^-, Br^-, I^-, OAc^-, OH^-, NO_2^-, NO_3^-, CO_3^{2-}, H_2O_2, HSO_4^-, HPO_4^-, PF_6^-, arginine, glutathione, cysteine and homocysteine. As shown in Fig. 2a, the addition of other anions had almost no influence on the absorption of the sensor **PHSH**. Evidently, only the presence of H_2S caused a distinct appearance of absorbance at 435 nm with an instant color change, as discussed above. The extent of absorption change at 435 nm was also compared with anions using a bar diagram (Fig. 2b).

Furthermore, to check the suitability of **PHSH** to detect H_2S quantitatively, systematic UV-vis titration was carried out. As shown in Fig. 3a, upon the successive incremental addition of H_2S to **PHSH** solution in acetonitrile: water (7:3) solvent medium, a gradual absorbance increase at 435 nm was observed. The absorption increase at 435 nm was about 38-fold and reached saturation over the addition of 2 equiv. of H_2S. Encouraged by the absorption results, we moved on to check the photoluminescence properties of **PHSH** before and after the addition of H_2S. However, **PHSH** did not exhibit any fluorescent properties. This could be due to the photo-induced electron transfer (PET) caused quenching. As the reaction between **PHSH** and H_2S leaves the probe with a free amino group, there could be possible PET form from amino group to phenanthridine core.

Besides, the plot of ΔA against the concentration of H_2S showed a linear relationship (Fig. 3b) with R^2 value of 0.9833. With the slope obtained from this linear equation and standard deviation (σ) from six blank measurements, we calculated the limit of detection (LOD) using the formula $3\sigma/K$. LOD of **PHSH** for H_2S was found to be 6.5 nM (Figure S5), which is comparable with the acceptable limit in the ambient environment proposed by U.S scientific advisory (<83 ppb) (77). As **PHSH** exerts optical change over the reaction between probe and H_2S,

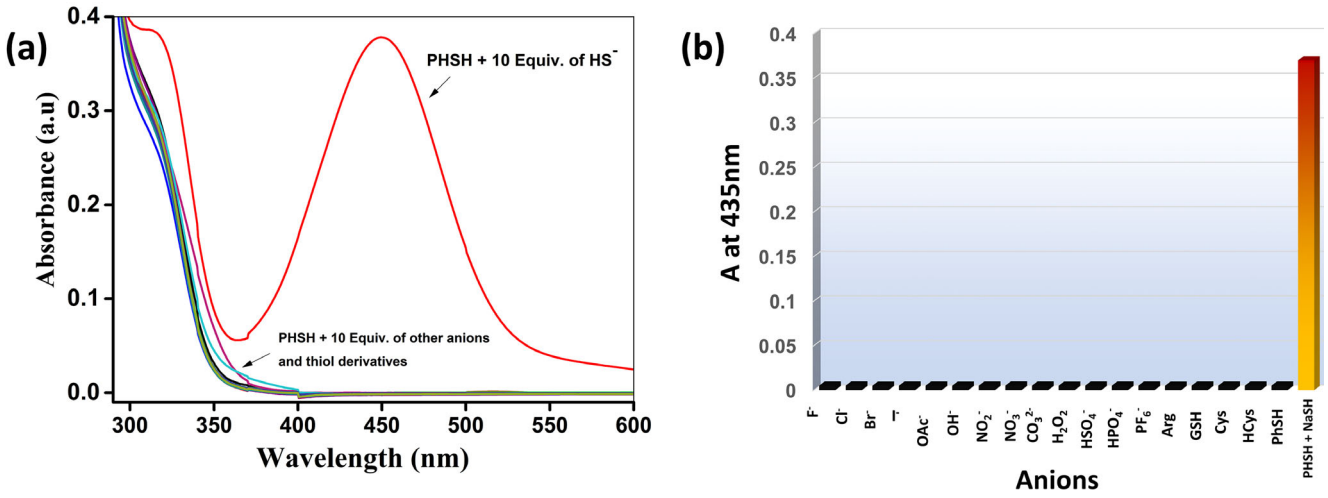

Figure 2. (a) UV-vis spectra of probe **PHBS** (2×10^{-6}) in acetonitrile: water (7:3) solvent medium upon addition of different anions and ligands. (b) Bar diagram which indicates variation of absorption intensity at 450nm over the addition of anions.

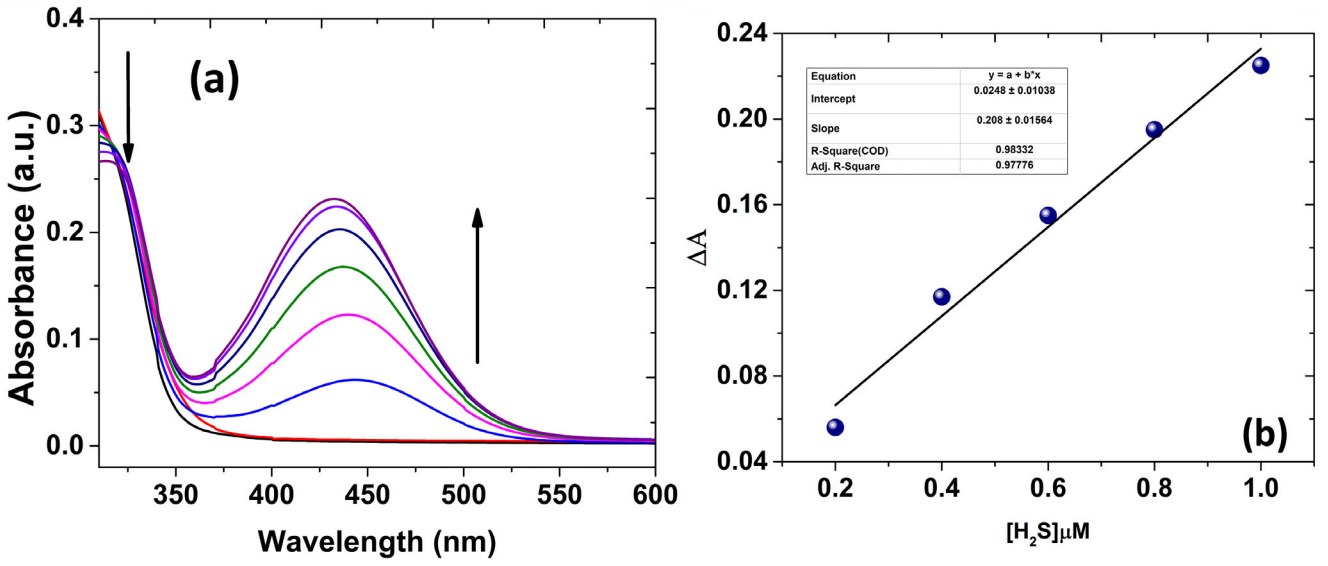

Figure 3. (a) Absorbance spectra of **PHBS** (1 μM) after incremental addition of H_2S up to 2 equiv. in acetonitrile: water (7:3) (v/v). (b) Absorption changes at 435 nm with increasing concentration of H_2S.

the reaction rate might affect the quality of the sensing (Figure S6). Hence, we investigated the influence of the reaction time on the probing results. From the temporal absorption tracking, we figured out that the absorption reached the plateau at 10 s, indicating that the concluding analytical results of H_2S detection can be achieved in a rapid manner.

Interference and the effect of pH

To establish uninterrupted detection of H_2S by **PHSH**, the dual anion cross tainting test was carried out, as shown in Fig. 4a. The competition experiments indicated the changes in the absorbance before and after adding H_2S into the **PHSH** solution with other anions (10 equiv.). **PHSH** was treated with two equiv. of H_2S in the presence of different anions, and it did not induce any substantial absorbance changes. This study revealed that **PHSH** could detect H_2S even in the presence of other potential competing anions. To study the practical applicability of probe **PHSH**, the effect pH was performed for **PHSH** and **PHSH+ H_2S** at various pH ranges to fix a particular pH to investigate real-time samples as they were found to appear in different pH ranges. It was found that for free **PHSH**, the absorption at 435 nm was insignificant and unperturbed at the pH ranges tested (pH = 2 to 12). For **PHSH+ H_2S,** under neutral and basic conditions, the absorbance had very little change. On the contrary, at acidic pH conditions (≤5), absorbance tended to decrease steadily with decreasing pH. These results demonstrated that **PHSH** could be used to detect H_2S under physiological and basic pH conditions. In addition, **PHSH+ H_2S** was found to exhibit emission at a lower pH value. This could be due to the inhibition of photo-induced electron transfer (PET) from the free

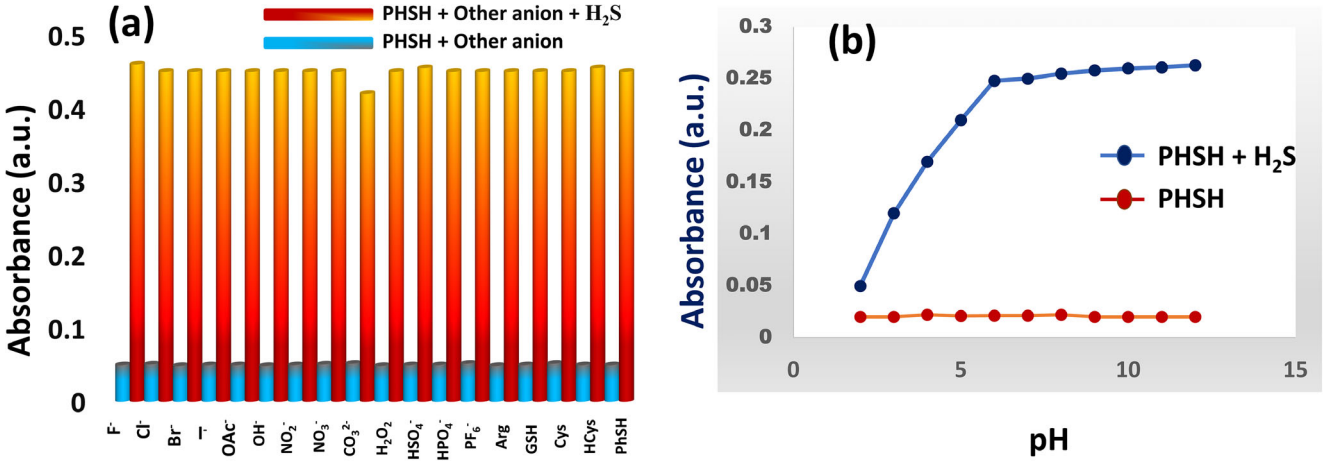

Figure 4. (a) Absorption response at 435 nm of free **PHBS** (2×10^{-6} M) and **PHBS+ H_2S** on addition of other anions (10 equiv.) (b) Effect of pH of free probe **PHBS** and **PHBS+ H_2S**.

amino group to phenanthridine due to the protonation of the free amino group, which resulted from the reaction between **PHSH** and H_2S.

Sensing mechanism

To further confirm that the colorimetric response was due to the H_2S-triggered thiolysis reaction of **PHSH** and the release of yellow free amino-containing compound (**PHN**) (Fig. 5), we recorded and compared ^{1}H NMR (in DMSO-*d6* solvent) of free **PHSH** in the presence of various levels of H_2S. The aromatic protons responsible for the aryl portion of 2,4- dinitrophenyl (H_a) started to vanish (δ = 9.18, 8.51, 8.49) steadily, and the new peaks (H_b) began to appear at (δ = 8.91, 8.58, 8.57), which was due to the release of 2,4-dinitrobenzenethiol by product. A new peak at δ 9.52 ppm started to form, indicating the formation of the free –NH_2 group. In addition, the thiolysis product was purified and subjected to HRMS analysis. The mass peak at m/z = 374.1769 confirmed the structure of **PHN** (Figure S7). High-performance liquid chromatography (HPLC)-based reaction monitoring was carried out for the reaction between **PHSH** and H_2S. Under the HPLC method used, **PHSH** had a retention time of 5.49 minutes with very high purity. When various levels of H_2S were allowed to react with **PHSH**, a new peak at 8.32 minutes started to appear due to the formation of **PHN** (Figure S8). Thus, the mechanism of probe **PHSH** for sensing H_2S is based on the thiolysis of the dinitrophenyl ether group.

Naked eye detection of H_2S by test strips

To simplify the detection process of H_2S, **PHSH** impregnated test strips were prepared by soaking filter papers in acetonitrile solution of **PHSH** (2 x 10^{-5} M), and the filter papers were air-dried before further analysis. As can be seen in Fig. 6a, test paper strips exhibited no color. After treating with various anions (those chosen in the optical study), only H_2S caused an obvious color change to yellow. Hence, **PHSH**-coated filter papers can be used as a qualitative testing tool for rapid onsite detection of H_2S. As shown in Fig. 6b, when the test paper was dipped in the solution of different concentrations of H_2S, the color of PHSH-coated filter paper gradually changed from colorless to yellow. These dip strips are quite helpful as an instant and low-cost tool for the qualitative detection of H_2S.

Practical application

The potential applicability of **PHSH** for the facile detection of H_2S was further extended to analyze real-time samples, such as water and food samples (Red wine, beer). The excessive presence of H_2S in wine and beer causes severe damage to the quality. Chosen and collected samples were spiked with the known concentration of H_2S and added to the solution of **PHSH**. The increase in the absorbance at 435 nm was investigated for the data analysis. As can be seen in Table 1, the spiked H_2S concentration was determined with satisfactory recovery in the range of 87.0 – 95%. These results indicated that this phenanthridine-based colorimetric probe could be a promising candidate for determining H_2S content in various real-time matrices and for quality control.

CONCLUSION

In summary, we have reported a new phenanthridine-based sensor **PHSH** with 2,4-dinitrobenzene sulfonyl group for the selective and sensitive detection of H_2S. When added with H_2S, **PHSH** showed rapid (within 10s) and remarkable absorption enhancement at 435 nm and responded to concentration at a level as low as LOD = 6.5 nM. Besides, the **PHSH** solution became dark yellow from colorless over the addition of H_2S. Sensor **PHSH** exhibits high selectivity for H_2S over other relevant thiols and anions in a semi aqueous solution. H_2S-triggered thiolysis of **PHSH** was confirmed by ^{1}H NMR and HRMS study. The potential real-time application of **PHSH** has been successfully demonstrated in various platforms, such as paper-based testing, analysis in different real-time matrixes. With the numerous advantages such as high sensitivity and selectivity, fast response time, ease of preparation and stability at a broad pH range, **PHSH** could stand as the ideal colorimetric chemosensor for H_2S.

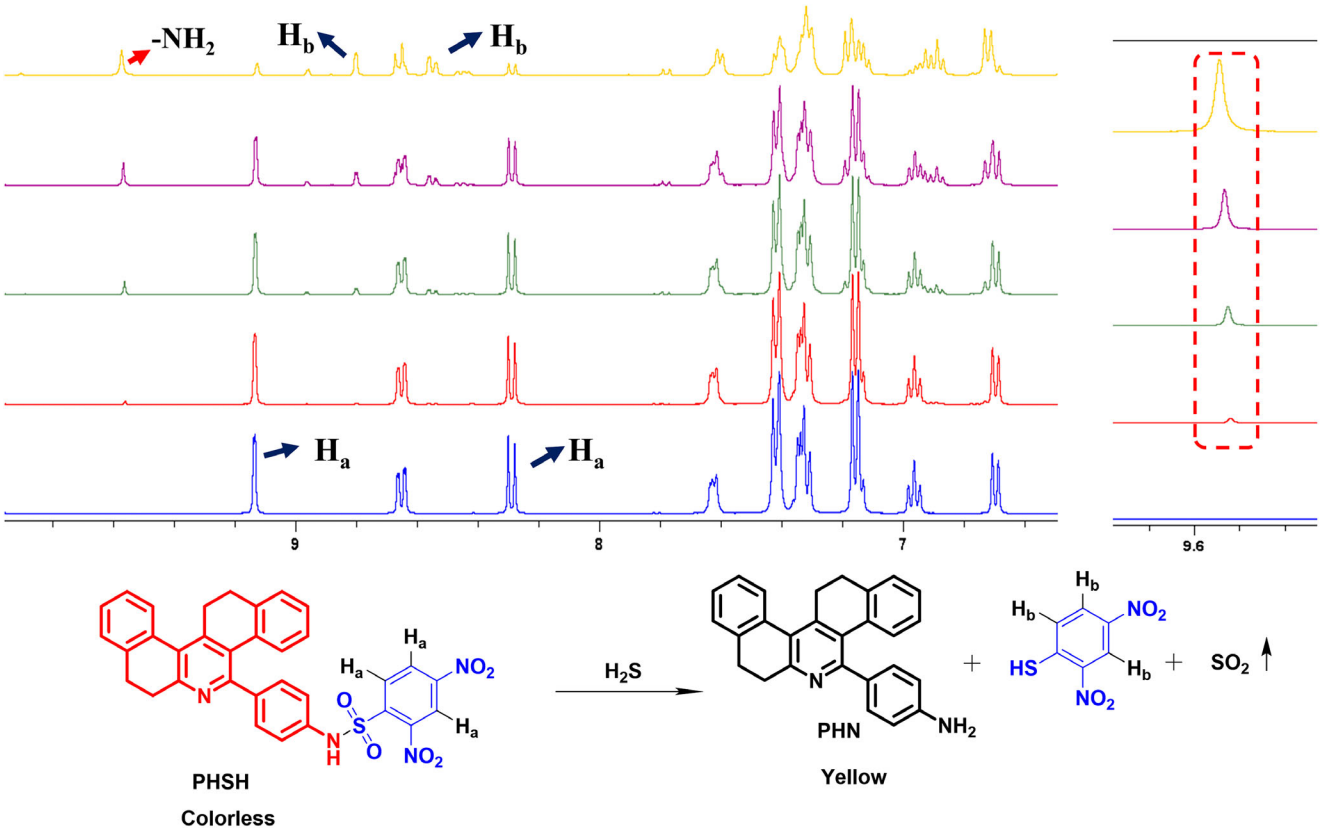

Figure 5. ^{1}H NMR titration spectra [400 MHz] of PHBS in DMSO-d6 at 25°C over the incremental addition of H_2S; Expansion of ^{1}H NMR region at 9–10 ppm; Reaction scheme indicating thiolysis of PHBS.

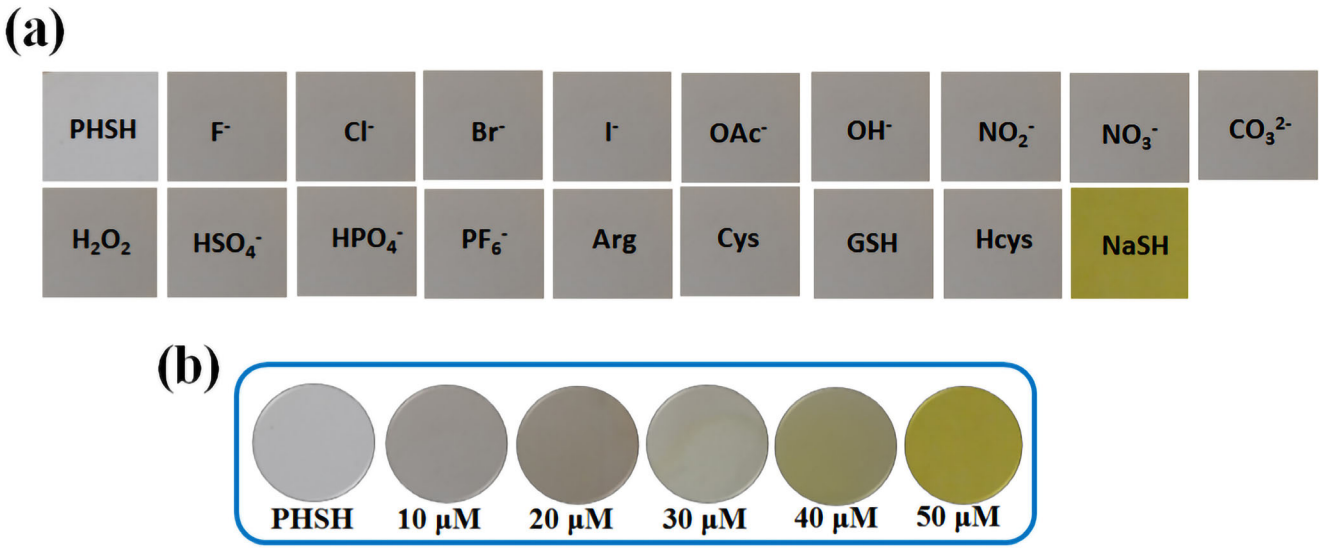

Figure 6. (a) Photograph showing naked eye visible color change of **PHBS** (2×10^{-5} M)-coated test paper strips after treating with various anions. (b) Photographs of **PHBS** (2×10^{-5} M)-coated test paper strips dipped into H_2S solutions (0, 10, 20, 30, 40 and 50 µM) under daylight.

Table 1. Determination of H_2S Concentrations in various real-time samples

Matrix	Spiked level (M)	Found level (M)	Recovery (%)	R.S.D† (n = 3) (%)
Tap water*	1×10^{-6}	0.92×10^{-6}	92	0.17
Lake water*	1×10^{-6}	0.89×10^{-6}	89	0.31
Well water*	1×10^{-6}	0.90×10^{-6}	90	0.27
Red wine	1×10^{-6}	0.88×10^{-6}	88	1.03
Beer	1×10^{-6}	0.87×10^{-6}	87	0.14

*Water samples were collected from in and around VIT campus, Vellore.
†Relative standard deviation.

Acknowledgements—Dhanapal J thanks VIT for providing financial support through research associateship. S M gratefully acknowledges the Youth 1000 Talent Program of China and Interdisciplinary Research Program of Hunan University. The DST-FIST NMR facility at VIT University is duly acknowledged. The authors thank Dr. R. Srinivasan, SSL-VIT, for language editing.

SUPPORTING INFORMATION

Additional supporting information may be found online in the Supporting Information section at the end of the article:

Figure S1. ^1H and ^{13}C NMR spectra of **(PHN)**.

Figure S2. ^1H and ^{13}C NMR spectra of **PHSH**.

Figure S3. HRMS spectra of **PHSN**.

Figure S4. Time-dependent stability analysis spectra of **PHSH**. Sensor probe PHSH 2 X 10^{-6} M solution prepared in acetonitrile: water (7:3) solvent medium

Figure S5. LOD determination of **PHSH** with H_2S. The calculated LOD of probe **PHSH** is 6.5 nM.

Figure S6. Effect of response time-dependent absorption spectrum of **PHSH** with **H_2S** in acetonitrile: water (7:3) solvent medium.

Figure S7. HRMS spectra of **PHSH** with H_2S.

Figure S8. HPLC-based reaction monitoring of **PHSH** with H_2S.

Table S1. Comparison of reported LOD value with PHSH for the detection of H_2S.

REFERENCES

1. Schiffman, S. S., J. L. Bennett and J. H. Raymer (2001) Quantification of odors and odorants from swine operations in North Carolina. *Agricult. Forest Meteorol.* **108**, 213–240.
2. Steve, W., H. R. Avery, S. W. Marshall, T. Kendall, T. Mansoureh, S. Leah and S. S. Schiffman (2008) Air pollution and odor in communities near industrial swine operations. *Environ. Health Perspect.* **116**, 1362–1368.
3. Franco-Luesma, E. and V. Ferreira (2016) Formation and release of h2s, methanethiol, and dimethylsulfide during the anoxic storage of wines at room temperature. *J. Agric. Food Chem.* **64**, 6317–6326.
4. Vela, E., P. Hernández-Orte, E. Franco-Luesma and V. Ferreira (2017) The effects of copper fining on the wine content in sulfur off-odors and on their evolution during accelerated anoxic storage. *Food Chem.* **231**, 212–221.
5. Duan, N., S. Yang, H. Tian and B. Sun (2021) The recent advance of organic fluorescent probe rapid detection for common substances in beverages. *Food Chem.* **358**, 129839.
6. Cheng, X., J. Gu, Y. Pang, J. Liu, T. Xu, X. Li, Y. Hua, K. A. Newell, X.-F. Huang, Y. Yu and Y. Liu (2019) Tacrine-hydrogen sulfide donor hybrid ameliorates cognitive impairment in the aluminum chloride mouse model of alzheimer's disease. *ACS Chem. Neurosci.* **10**, 3500–3509.
7. Kamoun, P., M.-C. Belardinelli, A. Chabli, K. Lallouchi and B. Chadefaux-Vekemans (2003) Endogenous hydrogen sulfide overproduction in Down syndrome. *Am. J Med. Genet. Part A* **116A**, 310–311.
8. Qian, L.-L., X.-Y. Liu, Q. Chai and R.-X. Wang (2018) Hydrogen sulfide in diabetic complications: focus on molecular mechanisms. *Endocrine, Metab. Immune Disord. - Drug Targets* **18**, 470–476.
9. Sun, H.-J., Z.-Y. Wu, X.-W. Nie, X.-Y. Wang and J.-S. Bian (2021) Implications of hydrogen sulfide in liver pathophysiology: mechanistic insights and therapeutic potential. *J. Adv. Res.* **27**, 127–135.
10. Sui, L., T. Yu, D. Zhao, X. Cheng, X. Zhang, P. Wang, Y. Xu, S. Gao, H. Zhao, Y. Gao and L. Huo (2020) In situ deposited hierarchical CuO/NiO nanowall arrays film sensor with enhanced gas sensing performance to H_2S. *J. Hazardous Mat.* **385**, 121570.
11. Wang, S., X. Liu and M. Zhang (2017) Reduction of Ammineruthenium(III) by sulfide enables in vivo electrochemical monitoring of free endogenous hydrogen sulfide. *Anal. Chem.* **89**, 5382–5388.
12. Asif, M., A. Aziz, Z. Wang, G. Ashraf, J. Wang, H. Luo, X. Chen, F. Xiao and H. Liu (2019) Hierarchical CNTs@CuMn layered double hydroxide nanohybrid with enhanced electrochemical performance in H_2S detection from live cells. *Anal. Chem.* **91**, 3912–3920.
13. Xu, T., N. Scafa, L.-P. Xu, S. Zhou, K. A. Al-Ghanem, S. Mahboob, B. Fugetsu and X. Zhang (2016) Electrochemical hydrogen sulfide biosensors. *Analyst* **141**, 1185–1195.
14. Paul, A., B. Schwind, C. Weinberger, M. Tiemann and T. Wagner (2019) Gas responsive nanoswitch: copper oxide composite for highly selective H_2S detection. *Adv. Funct. Mat.* **29**, 1904505.
15. Ullrich, S., S. K. Neef and H.-G. Schmarr (2018) Headspace solid-phase microextraction and gas chromatographic analysis of low-molecular-weight sulfur volatiles with pulsed flame photometric detection and quantification by a stable isotope dilution assay. *J. Sep. Sci.* **41**, 899–909.
16. Yu, Y., G. Li, D. Wu, F. Zheng, X. Zhang, J. Liu, N. Hu, H. Wang and Y. Wu (2020) Determination of hydrogen sulfide in wines based on chemical-derivatization-triggered aggregation-induced emission by high-performance liquid chromatography with fluorescence detection. *J. Agric. Food Chem.* **68**, 876–883.
17. Lynch, M. J. and B. R. Crane (2019) Design, validation, and application of an enzyme-coupled hydrogen sulfide detection assay. *Biochemistry* **58**, 474–483.
18. Alvarez, M. T., C. Crespo and B. Mattiasson (2007) Precipitation of Zn(II), Cu(II) and Pb(II) at bench-scale using biogenic hydrogen sulfide from the utilization of volatile fatty acids. *Chemosphere* **66**, 1677–1683.
19. Gong, D., X. Zhu, Y. Tian, S.-C. Han, M. Deng, A. Iqbal, W. Liu, W. Qin and H. Guo (2017) A phenylselenium-substituted BODIPY fluorescent turn-off probe for fluorescence imaging of hydrogen sulfide in living cells. *Anal. Chem.* **89**, 1801–1807.
20. Karakuş, E., M. Üçüncü and M. Emrullahoğlu (2016) Electrophilic cyanate as a recognition motif for reactive sulfur species: selective fluorescence detection of H_2S. *Anal. Chem.* **88**, 1039–1043.
21. Wang, M., Y. Song, P. Mu, X. Cai, Y. Lin and C.-L. Chen (2020) Peptoid-based programmable 2D nanomaterial sensor for selective and sensitive detection of H_2S in live cells. *ACS Appl. Bio Mater.* **3**, 6039–6048.
22. Jin, X., S. Wu, M. She, Y. Jia, L. Hao, B. Yin, L. Wang, M. Obst, Y. Shen, Y. Zhang and J. Li (2016) Novel fluorescein-based fluorescent probe for detecting H_2S and its real applications in blood plasma and biological imaging. *Anal. Chem.* **88**, 11253–11260.
23. Wu, Y., Q. Wang, T. Wu, W. Liu, H. Nan, S. Xu and Y. Shen (2018) Detection and imaging of hydrogen sulfide in lysosomes of living cells with activatable fluorescent quantum dots. *ACS Appl. Mater. Interfaces* **10**, 43472–43481.
24. Kaushik, R., R. Sakla, A. Ghosh, G. T. Selvan, P. M. Selvakumar and D. A. Jose (2018) Selective detection of H_2S by copper complex

embedded in vesicles through metal indicator displacement approach. *ACS Sens.* **3**, 1142–1148.
25. Li, H., Y. Fang, J. Yan, X. Ren, C. Zheng, B. Wu, S. Wang, Z. Li, H. Hua, P. Wang and D. Li (2020) Small-molecule fluorescent probes for H_2S detection: advances and perspectives. *TrAC Trends Analyt. Chem.* **134**, 116117.
26. Wu, S., X. Ma, Y. Wang, J. Zhou, X. Li and X. Wang (2021) A novel fluorescent BODIPY-based probe for detection of Cu^{2+} and H_2S based on displacement approach. *Spectrochim. Acta Part A: Mol. Biomol. Spectrosc.* **249**, 119330.
27. Li, K.-B., W.-B. Qu, Q. Shen, S. Zhang, W. Shi, L. Dong and D.-M. Han (2020) 1,8-Naphthalimide-based dual-response fluorescent probe for highly discriminating detection of cys and H_2S. *Dyes Pigments* **173**, 107918.
28. Nandi, S., H. Reinsch and S. Biswas (2020) A vinyl functionalized mixed linker CAU-10 metal-organic framework acting as a fluorescent sensor for the selective detection of H_2S and palladium(II). *Micropor. Mesopo. Mat.* **293**, 109790.
29. Ma, C., C. Wei, X. Li, X. Zheng, B. Chen, M. Wang, P. Zhang and X. Li (2019) A mitochondria-targeted dual-reactable fluorescent probe for fast detection of H_2S in living cells. *Dyes Pigments* **162**, 624–631.
30. Zhao, Q., J. Kang, Y. Wen, F. Huo, Y. Zhang and C. Yin (2018) "Turn-on" fluorescent probe for detection of H_2S and its applications in bioimaging. *Spectrochim. Acta Part A: Mol. Biomol. Spectrosc.* **189**, 8–12.
31. Wang, F., G. Xu, X. Gu, Z. Wang, Z. Wang, B. Shi, C. Lu, X. Gong and C. Zhao (2018) Realizing highly chemoselective detection of H_2S in vitro and in vivo with fluorescent probes inside core-shell silica nanoparticles. *Biomaterials* **159**, 82–90.
32. Zheng, H.-R., L.-Y. Niu, Y.-Z. Chen, L.-Z. Wu, C.-H. Tung and Q.-Z. Yang (2016) Cascade reaction-based fluorescent probe for detection of H_2S with the assistance of CTAB micelles. *Chinese Chem. Lett.* **27**, 1793–1796.
33. Palanisamy, S., L.-Y. Lee, Y.-L. Wang, Y.-J. Chen, C.-Y. Chen and Y.-M. Wang (2016) A water soluble and fast response fluorescent turn-on copper complex probe for H_2S detection in zebra fish. *Talanta* **147**, 445–452.
34. Kaushik, R., A. Ghosh and D. A. Jose (2016) Simple terpyridine based Cu(II)/Zn(II) complexes for the selective fluorescent detection of H_2S in aqueous medium. *J. Lumin.* **171**, 112–117.
35. Nandi, S., S. Banesh, V. Trivedi and S. Biswas (2018) A dinitro-functionalized metal–organic framework featuring visual and fluorogenic sensing of H_2S in living cells, human blood plasma and environmental samples. *Analyst* **143**, 1482–1491.
36. Cai, S., C. Liu, S. He, L. Zhao and X. Zeng (2020) Mitochondria-targeted fluorescent probe for imaging endogenous hydrogen sulfide in cellular antioxidant stress. *Anal. Methods* **12**, 5061–5067.
37. Jiménez, D., R. Martínez-Máñez, F. Sancenón, J. V. Ros-Lis, A. Benito and J. Soto (2003) A new chromo-chemodosimeter selective for sulfide anion. *J. Am. Chem. Soc.* **125**, 9000–9001.
38. El Sayed, S., M. Milani, M. Licchelli, R. Martínez-Máñez and F. Sancenón (2015) Hexametaphosphate-capped silica mesoporous nanoparticles containing cuii complexes for the selective and sensitive optical detection of hydrogen sulfide in water. *Chem. – A. Eur. J.* **21**, 7002–7006.
39. Wang, L., X. Chen and D. Cao (2017) A nitroolefin functionalized DPP fluorescent probe for the selective detection of hydrogen sulfide. *New J. Chem.* **41**, 3367–3373.
40. Naha, S., S.-P. Wu and S. Velmathi (2020) Naphthalimide based smart sensor for CN^-/Fe^{3+} and H_2S. Synthesis and application in RAW264.7 cells and zebrafish imaging. *RSC Adv.* **10**, 8751–8759.
41. Katla, J. and S. Kanvah (2018) Styrylisoxazole-based fluorescent probes for the detection of hydrogen sulfide. *Photochem. Photobiol. Sci.* **17**, 42–50.
42. Yang, L., Y. Zhang, X. Ren, B. Wang, Z. Yang, X. Song and W. Wang (2020) Fluorescent detection of dynamic H_2O_2/H_2S redox event in living cells and organisms. *Anal. Chem.* **92**, 4387–4394.
43. Li, S.-J., Y.-F. Li, H.-W. Liu, D.-Y. Zhou, W.-L. Jiang, J. Ou-Yang and C.-Y. Li (2018) A dual-response fluorescent probe for the detection of viscosity and H_2S and its application in studying their cross-talk influence in mitochondria. *Anal. Chem.* **90**, 9418–9425.
44. Lv, L., W. Luo and Q. Diao (2021) A novel ratiometric fluorescent probe for selective detection and imaging of H_2S. *Spectrochim. Acta Part A: Mol. Biomol. Spectrosc.* **246**, 118959.
45. Liu, K., C. Liu, H. Shang, M. Ren and W. Lin (2018) A novel red light emissive two-photon fluorescent probe for hydrogen sulfide (H_2S) in nucleolus region and its application for H_2S detection in zebrafish and live mice. *Sens. Actuators B: Chem.* **256**, 342–350.
46. Sun, Y., C. Li, X. Feng, C. Wang, N. Wang, J. Zhu, T. Wang and X. Cui (2021) Si-coumarin-based fluorescent probes for ultrafast monitoring H_2S in vivo. *Dyes Pigments* **186**, 109059.
47. Shi, X., C. Yin, Y. Wen and F. Huo (2019) A dual-sites fluorescent probe based on symmetric structure of naphthalimide derivative to detect H2S. *Dyes Pigments* **165**, 38–43.
48. Muthusamy, S., K. Rajalakshmi, Q. Xu, Y. Chen, L. Zhao and W. Zhu (2020) An azido coumarin-quinoline conjugated fluorogenic dye: utilizing amide-iminol tautomerism for H_2S detection in live MCF-7 cells. *Spectrochim. Acta Part A: Mol. Biomol. Spectrosc.* **238**, 118345.
49. Chen, B., J. Huang, H. Geng, L. Xuan, T. Xu, X. Li and Y. Han (2017) A new ESIPT-based fluorescent probe for highly selective and sensitive detection of hydrogen sulfide and its application in live-cell imaging. *New J. Chem.* **41**, 1119–1123.
50. Lee, S., D.-B. Sung, J. S. Lee and M. S. Han (2020) A fluorescent probe for selective facile detection of H_2S in serum based on an albumin-binding fluorophore and effective masking reagent. *ACS Omega* **5**, 32507–32514.
51. Yang, L., Y. Su, Y. Geng, Y. Zhang, X. Ren, L. He and X. Song (2018) A triple-emission fluorescent probe for discriminatory detection of cysteine/homocysteine, glutathione/hydrogen sulfide, and thiophenol in living cells. *ACS Sens.* **3**, 1863–1869.
52. Zhong, K., S. Zhou, X. Yan, X. Li, S. Hou, L. Cheng, X. Gao, Y. Li and L. Tang (2020) A simple H_2S fluorescent probe with long wavelength emission: application in water, wine, living cells and detection of H_2S gas. *Dyes Pigments* **174**, 108049.
53. Hong, J., E. Zhou, S. Gong and G. Feng (2019) A red to near-infrared fluorescent probe featuring a super large Stokes shift for light-up detection of endogenous H_2S. *Dyes Pigm.* **160**, 787–793.
54. Zhao, X., Y. Li, Y. Jiang, B. Yang, C. Liu and Z. Liu (2019) A novel "turn-on" mitochondria-targeting near-infrared fluorescent probe for H_2S detection and in living cells imaging. *Talanta* **197**, 326–333.
55. Liu, Y., Y. Ding, J. Huang, X. Zhang, T. Fang, Y. Zhang, X. Zheng and X. Yang (2017) A benzothiazole-based fluorescent probe for selective detection of H_2S in living cells and mouse hippocampal tissues. *Dyes Pigments* **138**, 112–118.
56. Fang, T., X.-D. Jiang, C. Sun and Q. Li (2019) BODIPY-based naked-eye fluorescent on-off probe with high selectivity for H_2S based on thiolysis of dinitrophenyl ether. *Sens. Actuators B: Chem.* **290**, 551–557.
57. Peng, S., T. Zhong, T. Guo, D. Shu, D. Meng, H. Liu and D. Guo (2018) A novel fluorescent probe for selective detection of hydrogen sulfide in living cells. *New J. Chem.* **42**, 5185–5192.
58. Guria, U. N., K. Maiti, S. S. Ali, S. K. Samanta, D. Mandal, R. Sarkar, P. Datta, A. K. Ghosh and A. K. Mahapatra (2018) Reaction-based bi-signaling chemodosimeter probe for selective detection of hydrogen sulfide and cellular studies. *New J. Chem.* **42**, 5367–5375.
59. Qian, M., L. Zhang, Z. Pu, J. Xia, L. Chen, Y. Xia, H. Cui, J. Wang and X. Peng (2018) A NIR fluorescent probe for the detection and visualization of hydrogen sulfide using the aldehyde group assisted thiolysis of dinitrophenyl ether strategy. *J. Mater. Chem. B* **6**, 7916–7925.
60. Xu, L., L. Ni, L. Sun, F. Zeng and S. Wu (2019) A fluorescent probe based on aggregation-induced emission for hydrogen sulfide-specific assaying in food and biological systems. *Analyst* **144**, 6570–6577.
61. Zhao, Y., M. M. Cerda and M. D. Pluth (2019) Fluorogenic hydrogen sulfide (H_2S) donors based on sulfenyl thiocarbonates enable H_2S tracking and quantification. *Chem. Sci.* **10**, 1873–1878.
62. Gong, S., E. Zhou, J. Hong and G. Feng (2019) Nitrobenzoxadiazole ether-based near-infrared fluorescent probe with unexpected high selectivity for H_2S imaging in living cells and mice. *Anal. Chem.* **91**, 13136–13142.

63. Zhang, J., G. Wen, W. Wang, K. Cheng, Q. Guo, S. Tian, C. Liu, H. Hu, Y. Zhang, H. Zhang, L. Wang and H. Sun (2020) Controllable cleavage of C-N bond-based fluorescent and photoacoustic dual-modal probes for the detection of H_2S in living mice. *Bio Mater, ACS Appl*. **4**, 2020–2025.
64. Ding, S., W. Feng and G. Feng (2017) Rapid and highly selective detection of H_2S by nitrobenzofurazan (NBD) ether-based fluorescent probes with an aldehyde group. *Sens. Actuators B: Chem.* **238**, 619–625.
65. Yi, L. and Z. Xi (2017) Thiolysis of NBD-based dyes for colorimetric and fluorescence detection of H_2S and biothiols: design and biological applications. *Org. Biomol. Chem.* **15**, 3828–3839.
66. Liu, G., H. Ge, R. Yin, L. Yu, C. Sun, W. Dong, Z. Sun, K. A. Alamry, H. M. Marwani and S. Wang (2020) Carbon dots tailored with a fluorophore for sensitive and selective detection of hydrogen sulfide based on a ratiometric fluorescence signal. *Anal. Methods* **12**, 1617–1623.
67. Jiang, Y., X. Ji, C. Zhang, Z. Xi, L. Sun and L. Yi (2019) Dual-quenching NBD-based fluorescent probes for separate detection of H_2S and Cys/Hcy in living cells. *Org. Biomol. Chem.* **17**, 8435–8442.
68. Tang, Y. and G.-F. Jiang (2017) A novel two-photon fluorescent probe for hydrogen sulfide in living cells using an acedan–NBD amine dyad based on FRET process with high selectivity and sensitivity. *New J. Chem.* **41**, 6769–6774.
69. Kaushik, R., A. Ghosh and D. Amilan Jose (2017) Recent progress in hydrogen sulphide (H_2S) sensors by metal displacement approach. *Coord. Chem. Rev.* **347**, 141–157.
70. Hartle, M. D., M. R. Tillotson, J. S. Prell and M. D. Pluth (2017) Spectroscopic investigation of the reaction of metallo-protoporphyrins with hydrogen sulfide. *J Inorg. Biochem.* **173**, 152–157.
71. Munusamy, S. and S. Kulathu Iyer (2016) A chiral (S)-BINOL based fluorescent sensor for the recognition of Fe(III) and cascade discrimination of α-amino acids. *Tetrahedron Asymmetry* **27**, 492–497.
72. Muthukumar, V., S. Munusamy, K. Thirumoorthy, S. Sawminathan and S. KulathuIyer (2019) Fused pyrazole-phenanthridine based dyads: synthesis, photo-physical and theoretical studies, and live cell pH imaging. *RSC Adv.* **9**, 38687–38696.
73. Munusamy, S., V. P. Muralidharan and S. K. Iyer (2017) Enantioselective recognition of unmodified amino acids by ligand-displacement assays with in situ generated 1:1 Cu(II)- BINOL imidazole complex. *Sens. Actuators B: Chem.* **250**, 244–249.
74. Munusamy, S. K., K. Thirumoorthy, V. P. Muralidharan, U. Balijapalli and S. K. Iyer (2017) Enantioselective fluorescent sensing of chiral carboxylic acid by engaging boronic acid and BINOL. *Sens. Actuators B: Chem.* **244**, 175–181.
75. Saravanakumar, M., B. Umamahesh, R. Selvakumar, J. Dhanapal, S. K. Ashok kumar and K. I. Sathiyanarayanan (2020) A colorimetric and ratiometric fluorescent sensor for biogenic primary amines based on dicyanovinyl substituted phenanthridine conjugated probe. *Dyes Pigments* **178**, 108346.
76. Sathiyanarayanan, K. I., N. S. Karthikeyan, P. G. Aravindan, S. Shanthi, R. S. Rathore and C. W. Lee (2009) Dual behavior of 2-tetralone: A new approach for the synthesis of 5-aryl-7,8,13,14-tetrahydrodibenzo[a, i]phenanthridine. *J. Heterocycl. Chemist.* **46**, 1142–1144.
77. Yu, T., X. Cheng, X. Zhang, L. Sui, Y. Xu, S. Gao, H. Zhao and L. Huo (2015) Highly sensitive H_2S detection sensors at low temperature based on hierarchically structured NiO porous nanowall arrays. *J. Mater. Chem. A* **3**, 11991–11999.